Noise in RF-CMOS Mixers: A Simple Physical Model

Hooman Darabi and Asad A. Abidi, *Fellow, IEEE*

***Abstract*—Flicker noise in the mixer of a zero- or low-intermediate frequency (IF) wireless receiver can compromise overall receiver sensitivity. A qualitative physical model has been developed to explain the mechanisms responsible for flicker noise in mixers. The model simply explains how frequency translations take place within a mixer. Although developed to explain flicker noise, the model predicts white noise as well. Simple equations are derived to estimate the flicker and white noise at the output of a switching active mixer. Measurements and simulations validate the accuracy of the predictions, and the dependence of mixer noise on local oscillator (LO) amplitude and other circuit parameters.**

***Index Terms*—Active mixers, CMOS integrated circuits, communication systems, integrated circuits, mixers, mixer noise, noise, nonlinear circuits, receivers.**

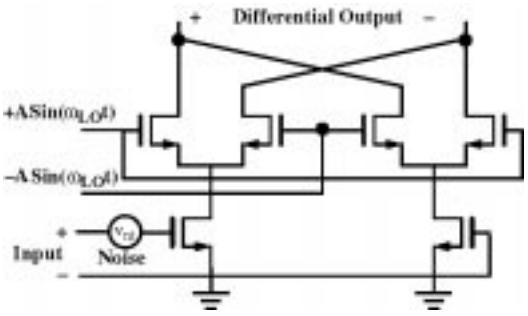

Fig. 1. A typical switching active mixer with noise source shown at the transconductor input.

I. Introduction

In THE course of design of a CMOS mixer, it was found that flicker ($1/f$) noise appears at its output even though the resistor loads are free of flicker noise. This is unexpected, because at first glance one expects flicker noise in the input stage transistors and mixer switches to translate in frequency. There are important repercussions in a direct-conversion receiver [1], where the signal downconverts to baseband after only minimal amplification at radio-frequency (RF). Mixer $1/f$ noise degrades signal-to-noise ratio (SNR), and as a consequence the overall noise figure of the receiver suffers. By using a modulation such as wideband FSK, it is sometimes possible to position the downconverted signal beyond the flicker noise corner [2]. However, there is no room to do so in a narrowband communication system such as FLEX used for wireless paging, where adjacent channels are only 25 kHz apart.

This paper describes the processes whereby flicker noise appears at the output of a CMOS downconversion mixer. Sometimes the noise is so large that it disqualifies the mixer for use in a direct-conversion receiver. In investigating these processes, a simple, qualitative model of noise in mixers has been developed whose predictions agree very well with sophisticated simulations of mixer noise, and with measurements. The model is extended to white noise. Straightforward equations capture the noise (both flicker and white) originating in different parts of the mixer. The main contribution of this work is to demystify mixer noise, which is so far dealt with in the literature using either exhaustive analyzes or specially developed simulation tools. We believe it should be as simple to estimate and optimize noise figure in mixers as it is in amplifiers.

Manuscript received January 27, 1999; revised September 8, 1999.

The authors are with the Department of Electrical Engineering, University of California, Los Angeles, CA 90095-1594 USA.

Publisher Item Identifier S 0018-9200(00)00122-0.

II. Low-Frequency Noise in a Mixer

An active mixer comprises an input transconductance, switches, and an output load. Noise is present in all the transistors making up these functions. First the noise contribution of the loads and transconductance FET's is described, followed by the noise contribution of the switches. Frequency translation of noise is dealt with approximately, using a simple analysis and qualitative reasoning. More accurate analytic [3] and numerical [4] methods have been presented elsewhere.

A. Load Noise

In a zero-IF receiver, flicker noise in the loads of the downconversion mixer competes with the signal [5]. This noise may be lowered in one of many ways. PMOSFET's show lower flicker noise [6], [7], ascribed to buried channel behavior, compared to NMOSFET's of the same dimensions. Therefore, PMOS loads may be used. Otherwise at the expense of some voltage headroom the mixer may be loaded with polysilicon resistors, which are free of flicker noise.

B. Transconductance Noise

A prototype CMOS transconductance mixer is shown in Fig. 1. Noise in the lower transconductance FET's accompanies the RF input signal, and is translated in frequency just like the signal is. Therefore, flicker noise in these FET's is upconverted to ω_{LO} and to its odd harmonics, while white noise at ω_{LO} (and its odd harmonics) is translated to DC. If the output of interest lies at zero IF, then the transconductance FET's only contribute white noise after frequency translation, since the flicker corner

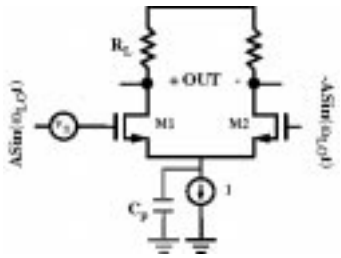

Fig. 2. Single-balanced mixer with switch noise modeled at gate.

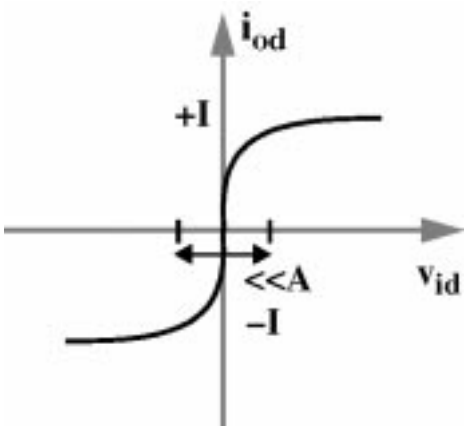

Fig. 3. Assumed switch I–V characteristic.

frequency of these devices is usually much lower than the LO frequency.

Due to mismatches in the switching transistor quad, a small amount of the flicker noise in the transconductance FET's can appear at the loads. This is dealt with at the end Section II-C.

C. Direct Switch Noise

Without loss of generality, consider the single-balanced mixer in Fig. 2. The bias current in the switch FET's M1 and M2 is periodic at a frequency $\omega_{\rm LO}$. Flicker noise arises from traps with much longer time constants than the typical period of oscillation at RF, and it may be assumed that the *time-average* inversion layer charge in the channel determines the root mean square (rms) flicker fluctuations. These charge fluctuations are referred as a voltage to the gate of one FET in the differential pair with a constant rms value and a spectral density proportional to $1/f$ (V_n in Fig. 2). This equivalent voltage is like a slowly varying offset voltage associated with differential pair. It should be noted that based on the carrier-density fluctuation model, the input referred flicker noise of MOSFET's is independent of V_{GS}. This bias independence is experimentally verified in NMOSFET's [6], [7].

To further simplify analysis, it is assumed that the circuit switches sharply, that is, a small differential voltage excursion (V_{id}) causes the current (i_{od}) to completely switch from one side of the differential pair to the other side (Fig. 3).

Now consider the direct effect of the switch noise at the mixer output. The transconductance RF input stage is replaced by a current source, I, at the tail. In the absence of noise, for positive values of LO voltage M1 switches ON and M2 switches OFF, and a current equal to I appears at the left branch. In the next

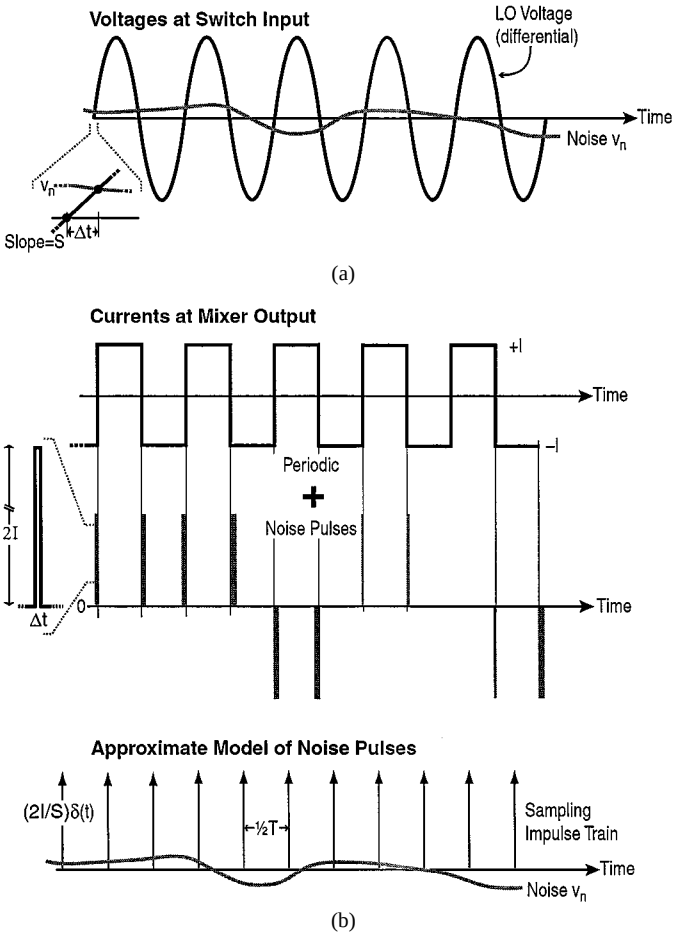

Fig. 4. (a) Switch input voltage and (b) mixer output current decomposed into noiseless response and pulse of noise.

half period, the current switches to the right branch. Thus, the output is a square-wave at frequency of $\omega_{\rm LO}$ with zero DC value. LO feedthrough is a characteristic of single-balanced mixers.

Next, include noise. The slowly varying V_n modulates the time at which the pair M1, M2 switches [Fig. 4(a)]. At every switching event the skew in switching instant modulates the differential current waveform at the mixer output. Although the *height* of the square-wave signal at the output remains constant, noise advances or retards the *time* of zero-crossing by $\Delta t = V_n(t)/S$, where S is the slope of the LO voltage at the switching time [Fig. 4(a)]. Now the waveform at the mixer output consists of a square-wave of frequency $\omega_{\rm LO}$ and amplitude I, representing the LO feedthrough, superposed with a pulse train of random widths Δt and amplitude of $2I$ at a frequency of $2\omega_{\rm LO}$, representing noise [Fig. 4(b)]. Over one period the average value of the output current is

$$i_{o,n} = \frac{2}{T} \times 2I \times \Delta t = \frac{2}{T} \times 2I \times \frac{V_n}{S} = 4I\frac{V_n}{S \times T} \qquad (1)$$

where T is the period of LO, equal to $2\pi/\omega_{\rm LO}$. This means that low-frequency noise at the gate of switch, V_n, appears at the output *without* frequency translation, and corrupts a signal downconverted to zero IF. The zero-crossing modulation, Δt, depends on the low-frequency noise, V_n, and the LO-voltage slope (S) at zero-crossing normalized to LO frequency, $S \times T$. For a sine-wave LO, $S \times T = 4\ \pi A$, where A is the amplitude

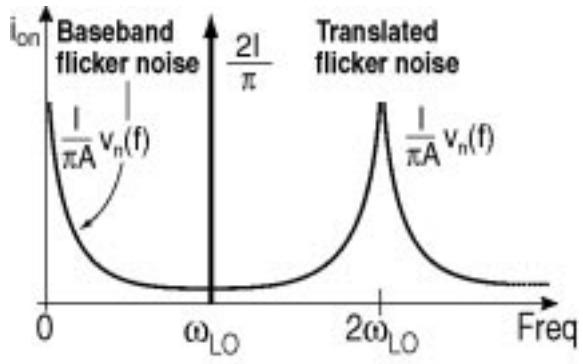

Fig. 5. Mixer output spectrum in presence of direct noise.

and a factor of two accounts for the fact that V_n is compared to a differential LO signal with an amplitude of $2A$.

It is instructive to examine the complete spectrum of the mixer output noise. As $\Delta t/T \ll 1$ the pulses are approximated with ideal delta-function impulses of amplitude $2I\Delta t/S$ at twice the LO frequency [Fig. 4(b)]. With this approximation, the spectrum is found by invoking well-known sampling theory: the noise waveform is scaled by $2I/S$, then impulse-sampled at a rate of $2\omega_{\rm LO}$ rad/s. The frequency spectrum of baseband noise current at the output is

$$i_{o,n}(f) = \frac{4I}{ST} V_n(f) = \frac{1}{\pi} \cdot \frac{I}{A} \cdot V_n(f) \tag{2}$$

where the last term applies to a sinewave LO of amplitude A. Sampled images of this spectrum appear at integer multiples of $2f_{\rm LO}$ (Fig. 5). At $f_{\rm LO}$, the LO feedthrough amplitude is equal to $2I/\pi$, which is independent of LO amplitude or switch size, but it has no flicker noise sidebands.

If the mixer is used for upconversion, the switches contribute no flicker noise to the output at $f_{\rm LO}$, although flicker noise in the transconductance stage is upconverted to this frequency.

Short channel MOSFET's obey the following I–V characteristic, which takes into account velocity saturation [8]

$$I = W v_{sat} C_{ox} \frac{V_{\rm eff}^2}{V_{\rm eff} + E_{sat} L} \tag{3}$$

where I is the drain current, $V_{\rm eff}$ is the transistor gate over-drive voltage ($V_{GS} - V_t$), W and L are the transistor channel width and length, respectively, C_{ox} is the gate oxide capacitance, v_{sat} is the saturated velocity, and E_{sat} is the saturated electric field. Hence, the ratio of the transconductance (g_m) to its DC bias current (I) is

$$\frac{g_m}{I} = \frac{2}{V_{\rm eff}} \cdot \frac{\frac{V_{\rm eff}}{2} + E_{sat} L}{V_{\rm eff} + E_{sat} L}. \tag{4}$$

In long channel transistors ($L \gg V_{\rm eff}/E_{sat}$), g_m/I approaches $2/V_{\rm eff}$ as predicted by the classic square-law. However, for short channel devices at large over-drive voltages, g_m/I approaches $1/V_{\rm eff}$. The short-channel formulas are used from here on.

These expressions are used to predict the SNR at the mixer output, which is also an indication of its noise figure. The gain from the RF input, $V_{\rm in}$, depends on I because the input FET transconductance is $I/(V_{GS} - V_t)$. As the conversion gain of a fully commutating mixer from RF input to the differential current output is $2/\pi \cdot g_m$, the SNR is

$$\mathrm{SNR}_1 = \frac{S \times T}{2\pi (V_{GS} - V_t)} \cdot \frac{V_{\rm in}}{V_n} = \frac{2A}{(V_{GS} - V_t)} \cdot \frac{V_{\rm in}}{V_n} \tag{5}$$

where the last term applies to a sinewave LO of amplitude A. This relationship shows that SNR improves by raising the product of the slope of the LO waveform at zero-crossing and its period (in the case of a sinewave LO, this amounts to raising A); by increasing the gate area of the switch FET's to lower flicker noise V_n; and by lowering the transconductance FET over-drive. However, increasing switch gate area or lowering $V_{GS} - V_t$ usually degrade mixer bandwidth.

The double-balanced mixer (Fig. 1) works in much the same way. The main difference is that there is no LO feedthrough, and V_n represents the equivalent noise of four switches in the mixer. V_n induces a pulse train with the width of Δt (as defined earlier) and frequency of $2\omega_{\rm LO}$ at the mixer output [Fig. 4(b)]. The low-frequency component of this waveform's spectrum is exactly equal to what was calculated in (1). Therefore, the noise at the output is the same as in (2).

This analysis also answers the earlier question of how flicker noise originating in the transconductance devices leaks through switch FET's unbalanced by an offset. Replace the noise voltage V_n with an offset voltage, V_{os}. The mixer output current is now a square-wave signal of *constant offset in its zero-crossings*, V_{os}/S, whose *height* is modulated by the noisy current, $I + g_{mi}.V_{ni}$, where V_{ni} is the input-referred flicker noise of the transconductance FET. In this case the output current has a constant DC offset equal to $(I.V_{os})/(\pi \cdot A)$ and a low-frequency noise component equal to

$$i_{o,n} = \frac{1}{\pi A} \cdot g_m \cdot V_{ni} \cdot V_{os}. \tag{6}$$

This is similar to (2), with I replaced by $g_m.V_{os}$. The corresponding SNR is

$$\mathrm{SNR}_2 = \frac{2A}{V_{os}} \cdot \frac{V_{\rm in}}{V_{ni}}. \tag{7}$$

If it is assumed in comparing (5) and (7) that the noise voltages are of a similar order of magnitude, then as $V_{os} \ll V_{GS} - V_t$, switch-induced noise is much larger than transconductance stage flicker noise leaking to the output due to DC offsets. In general, V_{ni} in (7) can represent any unwanted interference at the mixer input, such as low-frequency noise on the ground line.

D. Switch Noise: Indirect

The analysis so far suggests that flicker noise at the mixer output may be eliminated if the LO waveform is a perfect square-wave with infinite slope at zero crossing ((1)). However, as the LO *slope* rises, output flicker noise appears via another mechanism that depends on LO *frequency* and circuit capacitance. This is called the "indirect" mechanism.

Consider the mixer shown in Fig. 6, with a perfect square-wave applied to the LO port, alternating between voltages V_L and V_H. The voltage at the tail of the switching pair is V_s. In one half cycle of the LO, switch M1 is ON and M2 OFF. Therefore at the gate of transistor M1 a voltage V_H

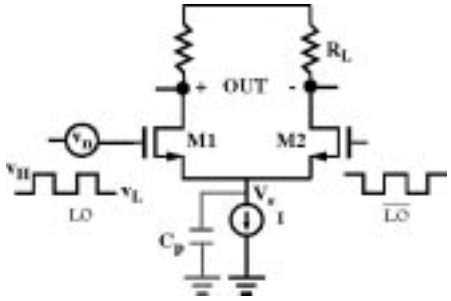

Fig. 6. Single-balanced mixer with a square-wave LO.

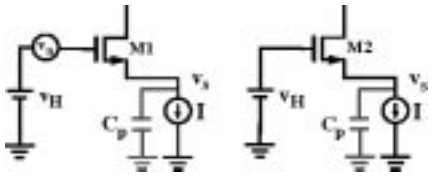

Fig. 7. Mixer with square-wave LO at each half cycle: (a) first half cycle and (b) second half cycle.

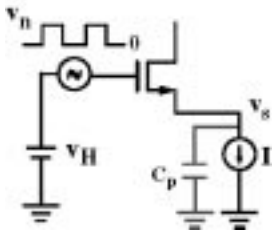

Fig. 8. Mixer in Fig. 6, replaced with a source follower.

is present in series with the noise source, V_n, as shown in Fig. 7(a). In the next half cycle, switch M2 is ON and now only the DC voltage, V_H, is at the gate [Fig. 7(b)]. Associating all the noise with one FET's gate correctly captures the differential noise in the switching pair.

To find the tail voltage, V_s, the hard-switched mixer is thought of as a single source follower continuously connected to the tail because of an assumed instantaneous crossover from M1 to M2, whose gate voltage alternates between zero and V_n around a bias V_H (Fig. 8).

The voltage at the tail, V_s, is estimated using a linear model because V_n is much smaller than the LO voltage, V_H, and because the source follower is relatively linear for large signals. Assuming that the transconductance is g_{ms}, the time constant at the source in Fig. 8 is C_P/g_{ms}, which is normally much smaller than the LO period, T. As a result, the tail voltage waveform charges exponentially to V_n at one half cycle, and discharges to zero in the other half cycle, as in Fig. 9(a).

This voltage produces the current waveform shown in Fig. 9(b) in the capacitance at the tail, C_P. The capacitive current, i_{Cp} has a frequency equal to the LO frequency, with zero DC value. At the mixer output in Fig. 6, when M1 is ON the differential current is i_{Cp}, while in the next half cycle, when M2 is ON, the output current commutates to $-i_{Cp}$, [Fig. 9(c)]. The output current alternates at twice the LO frequency with non-zero dc value, which indicates that baseband flicker noise is present at

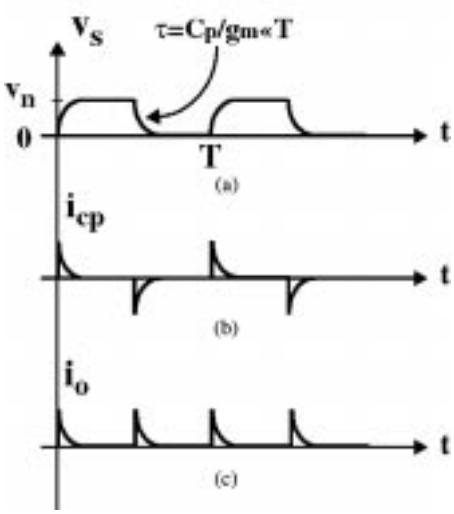

Fig. 9. Waveforms resulting from a square-wave LO: (a) voltage at tail, (b) capacitance current, and (c) output current.

the mixer output. The amount of $1/f$ noise is the average of the output current

$$i_{o,n} = \frac{2}{T}\int_0^{T/2} i_{Cp}(t)\,dt = \frac{2}{T}\int_0^{T/2} C_p\left[\frac{d}{dt}V_s(t)\right]\,dt. \tag{8}$$

Therefore the output noise current is

$$i_{o,n} = \frac{2}{T}C_p\left(V_s\left(\frac{T}{2}\right) - V_s(0)\right) = \frac{2}{T}C_pV_n. \tag{9}$$

The conversion gain to flicker noise in V_n due to the indirect process is $(2C_P)/T$. This gain grows with LO frequency, but is usually smaller than the gain due to the direct mechanism ((1)).

If the total capacitance at the tail is comparable to C_{GS} of the transconductance stage, then the SNR for indirect noise is given by

$$\mathrm{SNR}_3 = \frac{g_m\dfrac{2}{\pi}}{2f_{\mathrm{LO}}C_p} \times \frac{V_{\mathrm{in}}}{V_n} = 2\frac{f_T}{f_{\mathrm{LO}}}\cdot\frac{V_{\mathrm{in}}}{V_n} \tag{10}$$

where it is assumed that the switched mixer conversion gain is equal to $2/\pi$. Therefore, the effect of flicker noise at the mixer output can be reduced by applying a square-wave LO with sharp transitions and reducing the tail parasitic capacitance, or equivalently, increasing the unity current gain frequency of the transistors (f_T). When the junction capacitance of the transconductance stage dominates the total capacitance at the tail, increasing the size of switches improves the SNR since V_n goes down. However, when the capacitance of the switches dominates, then making the switches larger degrades the SNR since V_n is lowered as the square root, while f_T reduces linearly with channel length. Unlike the direct mechanism, now if the over-drive of the transconductance stage is reduced f_T decreases and SNR degrades.

When a sine-wave LO is applied to the mixer, the source follower model of Fig. 8 remains valid with the difference that its gate voltage consists of the switched noise super-imposed on a

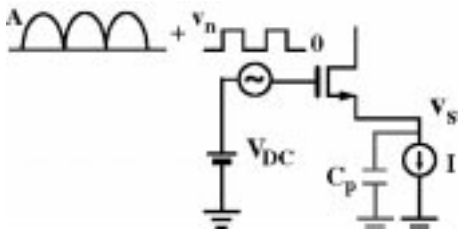

Fig. 10. Indirect mechanism for a sine-wave LO.

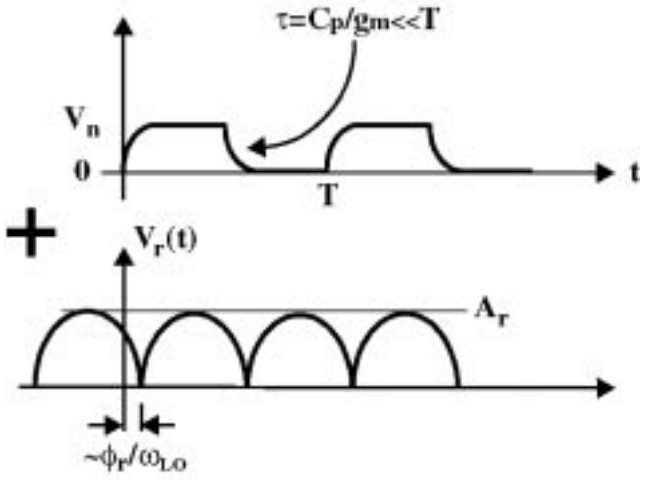

Fig. 11. Waveform at switching pair tail due to a sine-wave LO.

full-wave rectified sine-wave with a peak equal to the LO amplitude (Fig. 10). The rectified sine-wave captures the action of the alternating source followers; the tail voltage follows the gate with the larger voltage. Again, the tail voltage waveform (V_s) is estimated by superposing two signals, consisting of the exponentially charging/discharging V_n [Fig. 9(a)] and a large rectified sine-wave (V_r) whose amplitude is

$$A_r = A \cdot \frac{g_{ms}}{\sqrt{g_{ms}^2 + (C_p\omega_{\rm LO})^2}} \tag{11}$$

and whose phase difference with respect to the LO is

$$\phi_r = \text{atan}\left(\frac{C_P\omega_{\rm LO}}{g_{ms}}\right) \tag{12}$$

where A is the LO amplitude and g_{ms} is the switch transconductance. Fig. 11 shows the resultant voltage waveform at the source.

After downconversion, the exponential waveform leads to a noise component at the mixer output as calculated earlier and given in (9). The rectified sine-wave is downconverted by a noisy LO, consisting of a perfectly periodic square-wave and a train of pulses at twice the LO frequency, with a height equal to 2 but a width modulated by noise [Fig. 4(b)]. The height of the noisy pulses in Fig. 4(b) is $2I$, since these pulses downconvert the tail bias current (I).

The current produced in the tail capacitance by the rectified sine-wave, after downconversion by the noisy LO (train of pulses), has an average value of

$$\begin{aligned} i_{o,n} &= \frac{2}{T} \times 2 \times \int_{-(\Delta t/2)}^{\Delta t/2} C_P \left[\frac{d}{dt} V_r(t)\right] dt \\ &= \frac{4}{T} C_P \left(V_r\left(\frac{\Delta t}{2}\right) - V_r\left(-\frac{\Delta t}{2}\right)\right) \end{aligned} \tag{13}$$

where Δt is equal to V_n/S, as calculated before, and V_r is the rectified sine-wave at tail. This also contributes to the low-frequency noise at the mixer output. Notice the similarity of the above equation to the one derived for direct noise in Section II-C. If the capacitive current [the term $C_p\, d/dt V_r(t)$ in (13)] is replaced by the constant tail current, I, the result is exactly the same obtained in (1) for direct noise. After some simplifications in (13), the low-frequency noise spectrum at the mixer output is

$$i_{o,n}(f) = -\frac{2C_p}{T} V_n(f) \cdot \frac{g_{ms}^2}{g_{ms}^2 + (C_p\omega_{\rm LO})^2}. \tag{14}$$

This has the opposite sign to the term arising from the square-wave noise, given in (9). The total noise at the output is the sum of the two components, given in (9) and (14)

$$i_{o,n} = \frac{2C_p}{T} V_n \cdot \frac{(C_p\omega_{\rm LO})^2}{g_{ms}^2 + (C_p\omega_{\rm LO})^2}. \tag{15}$$

When $\omega_{\rm LO} \ll g_{ms}/C_P$, the noise due to indirect mechanism is negligible for a sine-wave LO. However, it rapidly goes up as the tail capacitance increases. Downconversion of the switched noise at the tail by the noisy LO results in a second-order output, and is neglected.

In most practical situations, then, flicker noise due to a sine-wave LO is attributable to the direct mechanism, which is frequency *independent*. However, even a LO waveform with infinitely fast risetime and falltime does not eliminate flicker noise but pushes it down to a level determined by the tail capacitance. In general, LO waveforms with a large $S \times T$ product, that is, a low-frequency LO with sharp transitions will lower flicker noise.

III. High Frequency Noise in a Mixer

A. White Noise in Mixer Switches

The model developed to understand the origins of flicker noise at the mixer output is now extended to white noise in the switches. Starting with the direct mechanism, the noise current at the output [Fig. 12(a)] consists of train of pulses, with a rate of twice the LO frequency, with a height equal to $2I/S$ and a width randomly modulated by noise. To simplify analysis, this is approximated by a train of perfect rectangular pulses with some constant width of T_s and a height of $2I/(S.T_s)$, sampling the broadband noise V_n which fluctuates at rates comparable to, or greater than the LO frequency [Fig. 12(b)].

The width of each pulse in Fig. 12(b), T_s, is calculated from the I–V characteristic of the switching pair. Fig. 13(a) shows a simplified piecewise linear I–V curve which approximately

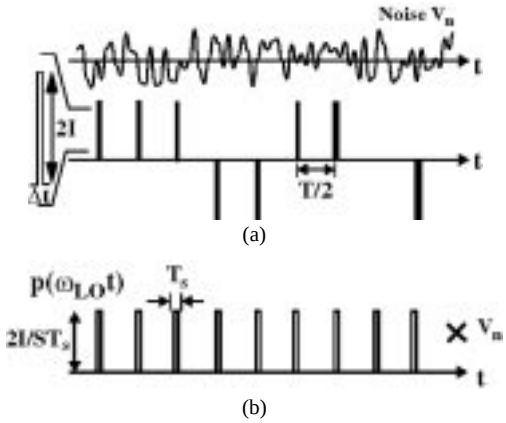

Fig. 12. (a) Noise current at the output and (b) output noise approximated by a train of pulses sampling the input noise.

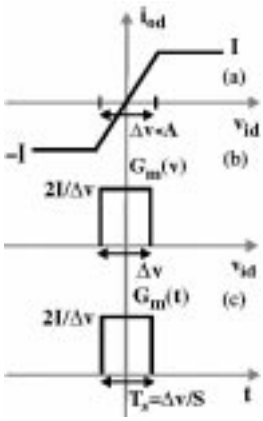

Fig. 13. (a) Switching pair I–V curve, (b) the transconductance of the switching pair in voltage domain, and (c) transconductance in time domain.

applies to any differential pair, independent of the detailed transistor characteristics. In a well-designed switching mixer the excursion ΔV is usually much smaller than the LO amplitude, A. The derivative of this characteristic [Fig. 13(b)] gives the bias dependent transconductance of the switching pair. For a sinewave LO $V_{id} = 2A\sin(\omega_{\rm LO}t)$, which produces a time-periodic transconductance, $G_m(t)$. G_m is then nonzero over the time window $\Delta V/2A\,\omega_{\rm LO} = \Delta V/S$ [Fig. 13(c)].

Switches contribute noise to the mixer output over the time when they are both ON. If one switch is OFF, it obviously contributes no noise, and neither does the other switch that is ON because it acts as a cascode transistor whose tail current is fixed to I by the RF input transconductance stage.

The sampling window, T_s, in Fig. 12(b), is the time when both switches are ON, that is $T_s = \Delta V/S$. This means that the switch noise, V_n, is transferred to the output only at each zero-crossing. The sampling function, $p(\omega_{\rm LO}t)$, can be expressed as

$$p(\omega_{\rm LO}t) = \sum_n G_m\left(t - \frac{nT}{2}\right) \tag{16}$$

where G_m is periodic at twice the LO frequency, since there are two zero-crossings over every cycle of the LO.

The mixer output noise

$$i_{o,n} = p(\omega_{\rm LO}t)\cdot V_n(t) \tag{17}$$

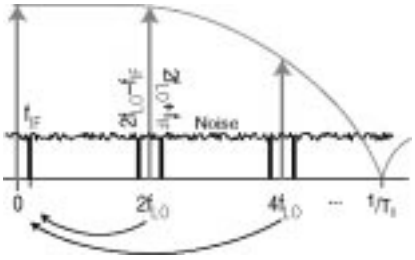

Fig. 14. Frequency translations of white noise originating in mixer switches.

which is *white* and *cyclostationary* can be expressed as the product of $p(\omega_{\rm LO}t)$, a *periodic* and *deterministic* sampling function, and V_n the *white* and *stationary* switch input-referred noise [10]. The autocorrelation of the output noise is calculated as

$$R_{i_{o,n}}(t+\tau, t) = p(t)\cdot p(t+\tau)\cdot R_{V_n}(\tau). \tag{18}$$

The autocorrelation of white noise, $R_{vn}(\tau)$, is a delta function. However, the output noise autocorrelation is a function of both t and τ, which indicates that the output noise is *not stationary* but periodic, proving that the output noise is white and cyclostationary, as expected. The power spectral density is calculated by averaging $R_{io,n}$ over one period and transforming the result, now only a function of τ, into the frequency domain [10], [11]. The power spectral density of the output current noise is

$$\hat{i^2_{o,n}} = \frac{2}{T}\int_0^{T_2} p^2(t)\,dt\cdot\hat{V_n^2} = \frac{2}{T}\cdot\left(\frac{2I}{S}\right)^2\cdot\frac{1}{T_s}\cdot\hat{V_n^2}. \tag{19}$$

The input noise is white and stationary and its power spectral density is

$$\hat{V_n^2} = \frac{4kT\gamma}{G_m} \tag{20}$$

where γ is the channel noise factor, traditionally 2/3 for long-channel MOSFET's, higher in practice due to hot carrier effects [9] (also it lumps other sources of noise in a transistor, such as back-gate noise), and G_m is the switch transconductance at zero-crossing

$$G_m = \frac{2I}{\Delta V}. \tag{21}$$

Combining (19)–(21), the power spectral density of the output current noise due to one switch is

$$\hat{i^2_{o,n}} = 4kT\gamma\frac{4I}{ST}. \tag{22}$$

When the LO waveform is a sine-wave, $S = 2A\omega_{\rm LO}$ and then

$$\hat{i^2_{o,n}} = 4kT\gamma\frac{I}{\pi A} \tag{23}$$

which says that the output noise density of switches only depends on LO amplitude and the bias current, and not on transistor size!

There is a physical explanation of this surprising result. The discrete sampling action at the zero-crossings aliases the broadband white noise of the switches (Fig. 14). The finite bandwidth of the sampling pulses, determined by the inverse

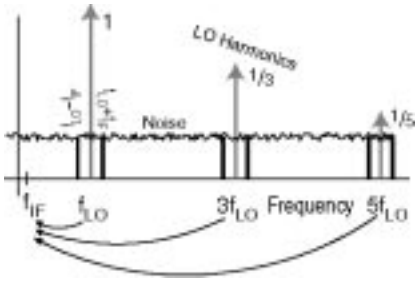

Fig. 15. Frequency translations of white noise originating in RF input transconductor.

of the time when both switches are on (T_s in Fig. 12), limits the number of aliases. In fact, the train of *finite pulses* in Fig. 12(b) may be replaced by a train of *impulses* (an ideal sampling function) passed through a filter with a sinc-shape frequency response, whose bandwidth is proportional to $1/T_s$ (the zeros of the sinc will lie at frequencies of N/T_s, where N =1, 2, 3, ...). Thus, with all else the same, as the switches get larger they turn ON for a shorter time and T_s decreases, widening the sampling bandwidth. However, as the switch size gets larger its input referred noise density is also lowered. The *integrated* rms output noise, therefore, remains constant, as does the equivalent white noise spectral density. This is similar to the well known integrated kT/C voltage noise on a switched capacitor, which is *independent* of the size of the switch.

Also, when some other external white and stationary noise source is present at the mixer LO port such as in LO buffers, its effect at the mixer output can be found by adjusting the noise factor, γ, in (20). Similarly, (17) can be applied to find the influence of any interferer in the LO port at the mixer output, where V_n will represent the interferer signal (the interferer should be, however, small relative to the LO magnitude so that the assumptions remain valid). An interferer at a frequency of f_i produces harmonics at the mixer output at f_i, $2f_{\rm LO} \pm f_i$, $4f_{\rm LO} \pm f_i$, ..., since $p(\omega_{\rm LO}t)$ is periodic at twice the LO frequency.

B. Transconductor Noise and Total Mixer Noise

With the noise due to the switches accounted for, what remains is the contribution of the transconductor stage to mixer output noise. As far as the mixer is concerned, white noise originating in the transconductor is indistinguishable from the RF input signal. Therefore, as mixer commutatation is assumed square wave-like, the LO frequency and its odd harmonics will downconvert the respective components of white noise to the IF (Fig. 15). After including the mixer conversion gain of $2/\pi$, the noise at IF is

$$\hat{V_{o,n}^2} = n \times \frac{4kT\gamma}{g_m} \cdot \left(\frac{2}{\pi}\, g_m R_L\right)^2. \tag{24}$$

The factor n in the last term represents accumulated noise after aliasing. *Any* periodic LO waveform, sine-wave or otherwise, which switches the mixer results in square-wave commutation of the transconductance stage output current. Therefore, using the well-known harmonic amplitudes of the square-wave

$$n = 2\left(1 + \frac{1}{3^2} + \frac{1}{5^2} + \cdots\right) = \frac{\pi^2}{4} \tag{25}$$

where the first term is the white noise at $\omega_{\rm LO} \pm \omega_{\rm IF}$ downconverted by the fundamental of the commutating waveform, the second term is noise at $3\omega_{\rm LO} \pm \omega_{\rm IF}$ downconverted by the third harmonic of the LO, whose amplitude is one third of the main harmonic, and so on. The noise is uncorrelated at each sideband and frequency, and the various contributions add as the mean square.

Including noise due to switches and the load, the total white noise at the mixer output is

$$\hat{V_{o,n}^2} = 8kTR_L + 8kT\gamma\frac{R_L^2 I}{\pi A} + n \times \frac{4kT\gamma}{g_m} \cdot \left(\frac{2}{\pi}\, g_m R_L\right)^2 \tag{26}$$

which simplifies to

$$\hat{V_{o,n}^2} = 8kTR_L\left(1 + \gamma\frac{R_L I}{\pi A} + \gamma\frac{g_m R_L}{2}\right) \tag{27}$$

where the first term is due to the two load resistors R_L, the second term is the output noise due to the *two* switches, and the third term shows the noise of the transconductance stage transferred to the mixer output, assuming a conversion gain of $2/\pi$.

This equation clearly shows how mixer output noise varies with different circuit parameters, such as LO amplitude (A) or mixer DC bias current (I). Most importantly, it allows the circuit designer to straightforwardly design the mixer to meet a target noise figure. In the double-balanced mixer there are twice as many FET's in the transconductance stage and the switches, so the output noise is

$$\hat{V_{o,n}^2} = 8kTR_L\left(1 + \gamma\frac{2R_L I}{\pi A} + \gamma g_m R_L\right) \tag{28}$$

where I is the bias current in each side of the mixer. Now compare a scaled double-balanced mixer with the same total current as a single-balanced mixer (that is, the former is biased at half the current per branch but the same $V_{GS} - V_t$ as the latter). The equations show that the output noise is the same for both mixers. However, since the gain of the double-balanced mixer from the differential input is half, the input referred noise voltage is twice as large. Referred to a differential 100 Ω source, its noise figure is 3 dB larger than that of a single-balanced mixer referred to a single-ended 50 Ω source resistance. The main advantage of the double-balanced mixer is that it suppresses LO feedthrough, as well as noise or interferers superimposed on the LO waveform applied to the mixer. It cannot suppress the uncorrelated noise in the switches.

C. Mixer Noise Optimization

The expression for total noise at the mixer output is expressed in terms of bias quantities by replacing g_m for a short channel MOSFET by $I/(V_{GS} - V_t)$, as discussed earlier

$$\hat{V_{o,n}^2} = 8kTR_L\left(1 + \gamma\,\frac{R_L I}{\pi A} + \gamma\frac{R_L I}{2(V_{GS} - V_t)}\right). \tag{29}$$

This shows that the relative noise contribution of the switches to the transconductance FET is $2(V_{GS} - V_t)/(\pi A)$. As the gate over-drive bias on the transconductance FET approaches the sine-wave LO amplitude, the switches, and transconductance

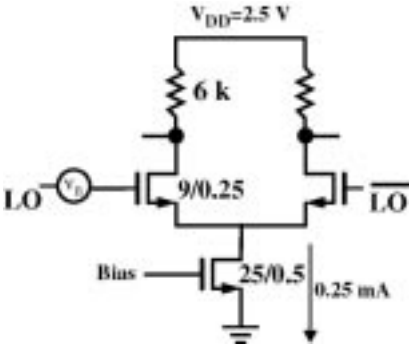

Fig. 16. Single-balanced mixer used in simulations.

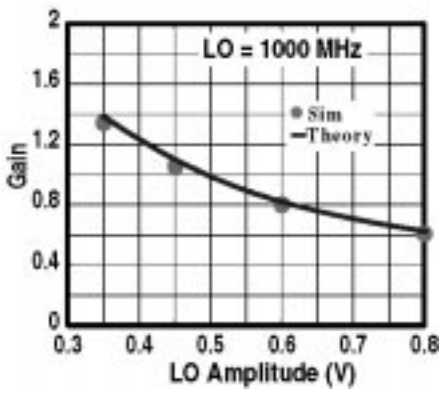

(a)

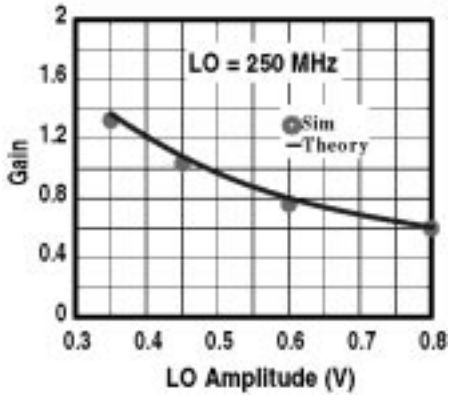

(b)

Fig. 17. Gain from noise port to output at: (a) 1 GHz and (b) 250 MHz.

stage contribute comparable noise at the mixer output. This is the fundamental tradeoff between noise and linearity in active mixers.

"Linear" mixers may bias the transconductance FET at a large over-drive to enhance the linearity, accompanied by modest LO swing to keep the switch transistors operating in saturation. These conditions boost the relative noise contribution of the switches. Also, as the DC voltage drop across the load resistor approaches the gate over-drive of the transconductance FET, the noise contribution of the load becomes more important.

Simple estimates of mixer noise sometimes neglect the contribution of the switches and load resistors, which underestimates noise figure by 2–4 dB. Also ignoring the aliasing of white noise in the transconductance underestimates noise figure by up to 1 dB [$\pi^2/4$ compared to 2 in (25)].

IV. Validating Theory by Simulation

To validate this theory a single-balanced mixer, shown in Fig. 16 is simulated using SPECTRE-RF at different LO frequencies and amplitudes. The FET's are described by Philips MOS model 9 parameters for the ST Microelectronics HCMOS7 process. A sine-wave voltage with an amplitude of 10 mV and frequency of 2 MHz models the low-frequency flicker noise at the gate of one of the switches (V_n). The amplitude of the output signal at 2 MHz is taken from the FFT of the output signal. The gain from the noise port to the output is then deduced.

The direct noise mechanism is simulated by applying a sine-wave LO with different amplitudes and frequencies, shown in Fig. 17. Very close agreement is seen between the simulations and theory. As predicted by (15), the gain at 1 GHz and 250 MHz is almost the same. The gain decreases as the LO amplitude goes up. At moderate LO swings, the gain from noise port to the output is almost unity, which means that the input-referred flicker noise of the switches can severely raise the mixer's noise floor at low frequencies.

Indirect noise is simulated by applying a perfect square-wave at the LO port. As seen in Fig. 18, simulations again agree closely with theory. In Fig. 18(a) when the tail capacitance increases beyond a certain value, the assumption that $C_P/g_m \ll T$ becomes invalid, and the theoretical curve deviates from the simulated gain. Fig. 18(b) shows that at 1 GHz, the voltage gain from the noise port to the mixer output is comparable to the gain due to the direct mechanism [Fig. 17(a)].

The white noise of the switches is also simulated using SPECTRE-RF periodic steady-state analysis, which can analyze noise of nonlinear circuits such as mixers. Fig. 19 compares the simulated output white noise of one switch with predictions based on (23), at different bias currents and LO amplitudes, for the mixer circuit of Fig. 16. The simulated noise is very close to predictions. Specifically, (23) predicts that noise is independent of switch size. To confirm this, mixer noise is simulated versus switch width and the results are plotted in Fig. 20. As the width varies from 4.5–18 μm, corresponding to about 100% variation in switch g_m, the white noise contributed by the switch to the mixer output changes only by 15%. This suggests that switches should be sized no further than large enough to turn on and off quickly for good mixer linearity, otherwise they lower mixer bandwidth and raise the load on the LO buffer without benefit of lower noise.

V. Measurement Results

The mixer shown in Fig. 21 was fabricated in the ST Microelectronics 0.25 μm CMOS process, and its output noise was measured. Measurements are now compared with theory and simulations. The flicker noise measurements are at an output frequency of 2.5 kHz, where the spectrum is clearly $1/f$. White noise is measured at about 1 MHz, where the spectrum is flat.

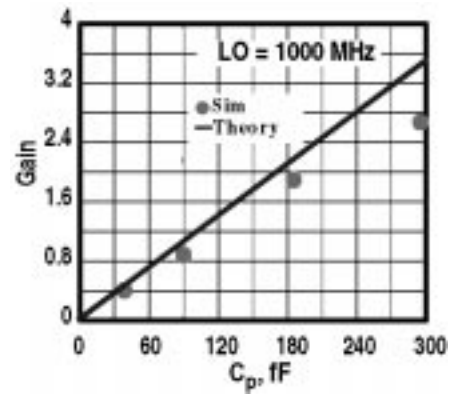

(a)

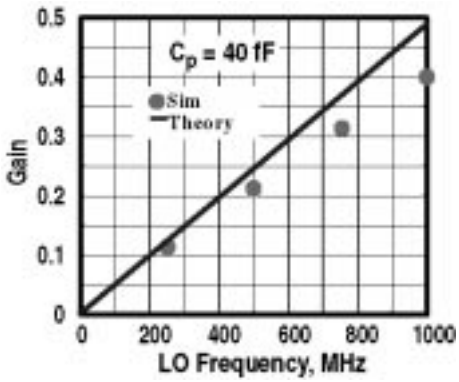

(b)

Fig. 18. Indirect noise at a constant: (a) frequency and (b) tail capacitance.

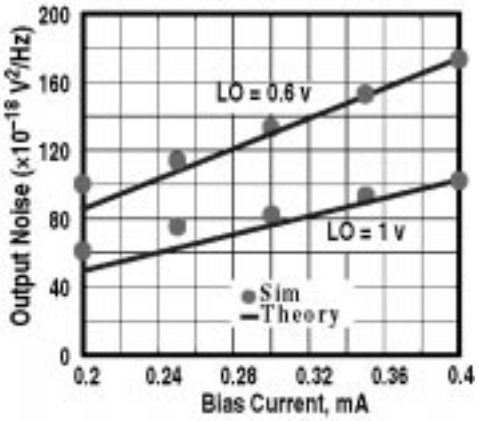

Fig. 19. Switch white noise at the mixer output for different LO amplitudes and bias currents.

The input referred flicker noise voltage of the switch FET's V_n is

$$V_{n,\mathrm{rms}} = \sqrt{2 \times \frac{K_f}{W_{\mathrm{eff}} \cdot L_{\mathrm{eff}} \cdot C_{ox} \cdot f}} \tag{30}$$

where

K_f = 1.2×10^{-24};
W_{eff} = 7.8 μm;
L_{eff} = 0.18 μm;
C_{ox} = 6.9 fF/μm^2;
f = 2.5 kHz.

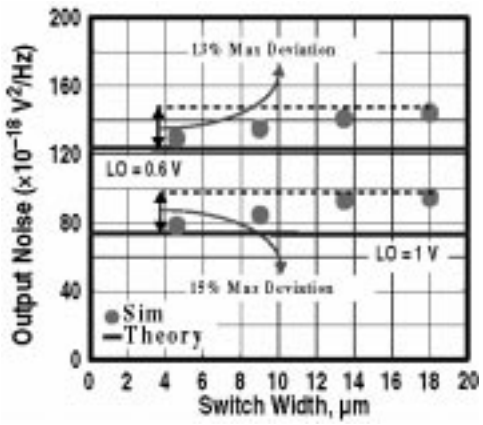

Fig. 20. Switch white noise versus its width.

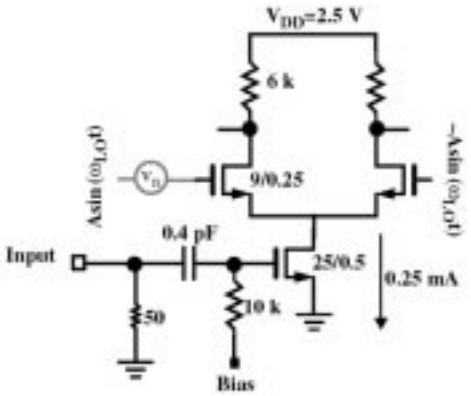

Fig. 21. Single-balanced mixer fabricated in ST HCMOS7 process.

The factor of two represents the uncorrelated noise of two switches. The value of K_f was initially predicted by scaling the results of actual flicker noise measurements done at UCLA [12]. Its exact value in this CMOS process was later extracted from actual noise measurements. Equation (30) leads to an input-referred flicker noise power spectral density for two switches of −117.1 dBm/Hz with respect to 50 Ω, which was then transferred to the output by the noise gain given in the plots of Fig. 17.

The output noise was also predicted using the periodic steady-state (PSS) noise simulation in SPECTRE-RF. The results of the output noise (with respect to 50 Ω) is shown in Fig. 22, for two frequencies of LO: 1000 and 250 MHz.

The simulations agree very well with theory. The flicker noise behavior of a mixer can be very simply calculated based on the equations presented here, and from knowledge of the device characteristics. In all cases, the noise level goes down as the LO amplitude increases. Measurements also match theory very well, with the largest discrepancy of 2.5 dB at the highest amplitude of the LO power. One possible source of this discrepancy is that both theory and Philips MOS 9 models assume that input-referred flicker noise is independent of bias. Any bias dependence in reality will be most pronounced in the measurements at large LO amplitudes.

Most of the flicker noise at the mixer output originates in the switches, since the load is free of flicker noise. Also very little flicker noise in the transconductance FET is expected to leak

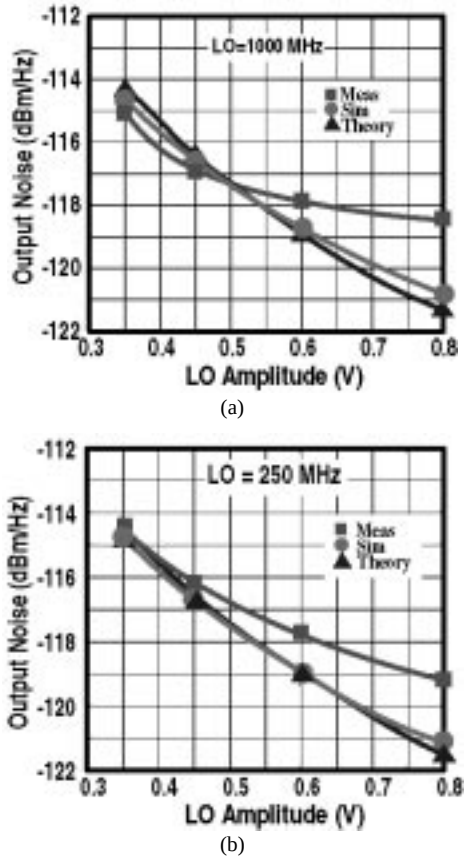

Fig. 22. Flicker noise at the mixer output at different LO amplitudes and frequencies: (a) LO = 1000 MHz and (b) LO = 250 MHz.

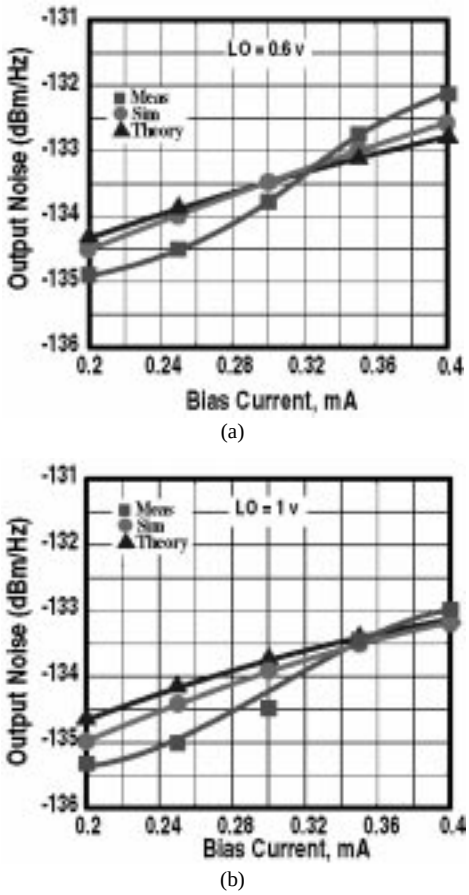

Fig. 23. White noise at the mixer output at different bias currents and LO amplitudes: (a) LO = 0.6 V and (b) LO = 1 V.

to the output in the measurements as the offset is much smaller than the bias $V_{GS} - V_t$.

The mixer white noise is measured at different bias currents and LO amplitudes, and compared to the theoretical white noise at the mixer output predicted by (27), and PSS simulations in SPECTRE-RF (Fig. 23). Again the measurement results are close to theory. A maximum error of about 1 dB between theory and measurements is seen, while the theory and SPECTRE-RF simulations agree to within a fraction of 1 dB.

VI. Conclusions and Discussion

This paper presents a simple but accurate model to predict flicker and white noise in mixers. By pinpointing the origins of the noise and the mechanisms of frequency translation, it allows the flicker noise to be optimized in a downconversion mixer intended for use at or near zero IF. The model uses the simplifying assumption that the switch FET's commutate instantly, and that the flicker noise of switches can be represented by a low-frequency *bias-independent* input voltage source. In spite of these apparently gross simplifications, good agreement is obtained with measurements. More complicated analytical methods using time-varying gain and stochastic concepts [3], or exhaustive analyzes [13] also deviate from measurements by as much as 2 dB. This analysis culminates in simple analytical expressions to capture mixer noise, analogous to well-known expressions for noise in an amplifier. The physical model is largely independent of transistor type, and may be applied to bipolar active mixers.

Switches in an active mixer contribute flicker noise to the mixer output in two different ways. One way, labeled *direct*, is by random modulation of the time instants of mixer switching. This contributes flicker noise at or near zero IF. Flicker noise is lower with sharper LO transitions relative to LO frequency. In the extreme case of a square-wave LO waveform with infinite slope, flicker noise at the mixer output does not disappear but may remain significant at GHz LO frequencies due to a newly discovered *indirect* mechanism. This noise grows smaller with lower LO frequency, or with higher device f_T and diminishing parasitic capacitances.

Although mixer flicker noise is only practically important in zero-IF or low-IF receivers, it is useful in probing all noise mechanisms in a time-varying circuit, because unlike white noise it does not accumulate after frequency translation, and therefore can be uniquely traced to the original sources at baseband.

The flicker noise model has been extended to evaluate white noise in the switches. Simple expressions are derived to capture the noise contribution of different sources in a switching mixer, requiring only basic circuit parameters, such as bias current, LO amplitude, and load resistance. White noise in switches sampled by pulses of nonzero width results in a kT/C-like expression for rms noise, which is independent of switch size. No complicated mathematical expression or MATLAB simulation is necessary.

Contrasted to previously reported methods [3], [13], the model presented here is specific to hard-switched commutating mixers, but it allows the noise to be predicted by a very simple equation. Obviously this is simple and flexible, and offers the circuit designer direct insights on mixer noise optimization and receiver frequency planning.

We believe that the method described here not only sheds light on mixers, but also on closely related circuits such as oscillators, which still lack a physical model to comprehensively explain their noise characteristics.

REFERENCES

[1] A. A. Abidi, "Direct-conversion radio transceivers for digital communications," *IEEE J. Solid-State Circuits*, vol. 30, pp. 1399–1410, Dec. 1995.

[2] A. Rofougaran, G. Chang, J. J. Rael, J. Y.-C. Chang, M. Rofougaran, P. J. Chang, M. Djafari, J. Min, E. W. Roth, A. A. Abidi, and H. Samueli, "A single-chip 900-MHz spread-spectrum wireless transceiver in 1-μm CMOS—Part II: Receiver design," *IEEE J. Solid-State Circuits*, vol. 33, pp. 535–547, Apr. 1998.

[3] C. D. Hull and R. G. Meyer, "A systematic approach to the analysis of noise in mixers," *IEEE Trans. Circuits and Systems—I: Fundamental Theory and Applications*, vol. 40, pp. 909–919, Dec. 1993.

[4] R. Telichevesky, K. Kundert, and J. White, "Receiver characterization using periodic small-signal analysis," in *Proc. Custom Integrated Circuits Conf.*, 1996, pp. 449–452.

[5] A. Rofougaran, J. Y. C. Chang, M. Rofougaran, and A. A. Abidi, "A 1 GHz CMOS RF front-end IC for a direct-conversion wireless receiver," *IEEE J. Solid-State Circuits*, vol. 31, pp. 880–889, July 1996.

[6] J. Chang, A. A. Abidi, and C. R. Viswanathan, "Flicker noise in CMOS transistors from subthreshold to strong inversion at various temperatures," *IEEE Trans. Electron Devices*, vol. 41, pp. 1965–1971, Nov. 1994.

[7] D. M. Binkley, J. M. Rochelle, B. K. Swann, L. G. Clonts, and R. N. Goble, "A micropower CMOS direct-conversion, VLF receiver chip for magnetic-field wireless applications," *IEEE J. Solid-State Circuits*, vol. 33, pp. 344–358, Mar. 1998.

[8] N. G. Einspruch and G. Gildenblat, "VLSI electronics microstructure science," in *Advanced MOS Device Physics*: Ney York: Academic, 1989, vol. 18.

[9] A. A. Abidi, "High frequency noise measurements on FET's with small dimensions," *IEEE Trans. Electron. Devices*, vol. ED-33, pp. 1801–1805, Nov. 1986.

[10] W. A. Gardner, *Cyclostationarity in Communications and Signal Processing*: Piscataway, NJ: IEEE Press, 1993.

[11] J. G. Proakis, *Digital Communications*: New York: McGraw Hill, 1995.

[12] J. J. Min, "Characterization of CMOS FET's flicker noise in VLSI technologies," masters dissertation, Dept. Elect. Eng., Univ. of California, Los Angeles, CA, 1988.

[13] M. T. Terrovitis and R. G. Meyer, "Noise in current-commutating CMOS mixers," *IEEE J. Solid-State Circuits*, vol. 34, pp. 772–783, June 1999.

Hooman Darabi was born in Tehran, Iran, in 1972. He received the B.S. and M.S. degrees in electrical engineering from Sharif University of Technology, Tehran, Iran, in 1994 and 1996, respectively. He received the Ph.D. degree from the University of California, Los Angeles, in 1999.

He is currently with Microlink Corporation, CA. His interests include analog and RF IC design for wireless communications.

Asad A. Abidi (S'80–M'81–SM'95–F'96) received the B.Sc.(Hon.) degree from Imperial College, London, in 1976 and the M.S. and Ph.D. degrees in electrical engineering from the University of California, Berkeley, CA, in 1978 and 1981, respectively.

He was with Bell Laboratories, Murray Hill, NJ, from 1981 to 1984 as a Member of the Technical Staff in the Advanced LSI Development Laboratory. Since 1985, he has been with the Electrical Engineering Department of the University of California, Los Angeles, where he is a Professor. He was a Visiting Faculty Researcher at Hewlett Packard Laboratories during 1989. His research interests are in CMOS RF design, high-speed analog integrated circuit design, data conversion, and other techniques of analog signal processing.

Dr. Abidi served as the Program Secretary for the International Solid-State Circuits Conference from 1984 to 1990, and as General Chairman of the Symposium on VLSI Circuits in 1992. He was Secretary of the IEEE Solid-State Circuits Council from 1990 to 1991, and from 1992 to 1995 he was an Editor of the IEEE JOURNAL OF SOLID-STATE CIRCUITS. He has received the 1988 TRW Award for Innovative Teaching and the 1997 IEEE Donald G. Fink Award, and was the corecipient of the Best Paper Award at the 1995 European Solid-State Circuits Conference, the Jack Kilby Best Student Paper Award at the 1996 International Solid-State Circuits Conference (ISSCC), the Jack Raper Award for Outstanding Technology Directions Paper at the 1997 ISSCC, and the Design Contest Award at the 1998 Design Automation Conference.